Colloid and Polymer Science (2021) 299:873–881
https://doi.org/10.1007/s00396-021-04810-z

ORIGINAL CONTRIBUTION

Phase behavior of solvent-rich compositions of the polymer/drug system poly(butylene succinate) and *N*,*N*-diethyl-3-methylbenzamide (DEET)

Hande Ece Yener[1] · Georg Hillrichs[2] · René Androsch[1]

Received: 30 October 2020 / Revised: 2 January 2021 / Accepted: 2 January 2021 / Published online: 19 January 2021

Abstract
Poly(butylene succinate) (PBS) is used to produce micro-/nanoporous biodegradable scaffolds, suitable for the release of the mosquito repellent *N*,*N*-diethyl-3-methylbenzamide (DEET), based on thermally induced phase separation. For solvent-rich compositions up to 30 m% PBS, it was found that PBS dissolves in DEET at elevated temperatures. During cooling, spherulitic crystallization of PBS occurs, with the crystallization temperature decreasing with the content of DEET and the cooling rate, as determined by cloud-point measurements, differential scanning calorimetry, and polarized-light optical microscopy. Scaffold morphologies of quenched solutions were analyzed by scanning electron microscopy as a function of the polymer concentration and the quenching temperature. These two parameters control the nucleus density/spherulite size, the degree of intermeshing of spherulites, and the intra- and interspherulitic pore size, with the latter typically being of the order of magnitude of few micrometers.

Keywords Poly(butylene succinate) (PBS) · *N*,*N*-Diethyl-3-methylbenzamide (DEET) · Solubility · Crystallization · Scaffold morphology

Introduction

Mosquito-borne diseases include malaria, dengue, West Nile fever, or yellow fever and affect a large proportion of the world population. Malaria cases exceeded 200 million in 2018 and caused more than 400,000 deaths, mostly in countries in Africa [1]. Mosquito repellents can help prevent the transmission of these diseases by reducing the contact between mosquitoes and humans. *N*,*N*-Diethyl-3-methylbenzamide (DEET) is a well-known mosquito repellent and considered as a gold standard among the many available repellents [2–4]. Studies showed that slow and controlled release of DEET from a carrier is an effective way to sustain protection from mosquito bites [5–10], however with possible carrier systems not yet sufficiently explored. This holds in particular for devices based on polymer scaffolds in which repellent is stored in open pores and slowly released to the environment.

In general, such polymer-based drug-release devices can be obtained by thermally induced phase separation (TIPS) during cooling of solutions with an upper critical solution temperature (UCST), as frequently demonstrated, e.g., for polylactides [11–16]. Depending on the crystallizability of the system components and the thermodynamic miscibility, TIPS may proceed via liquid-liquid (L-L) or solid-liquid (S-L) phase separation [17, 18]. In the latter case, the solution typically separates into solid polymer crystals and a liquid solvent-rich solution, which on further cooling may further separate into polymer-rich and solvent-rich phases when crossing the phase boundary line, or vitrify at the glass transition temperature of the solution.

Alternatively, a partially solid, phase-separated system may form via L-L TIPS followed by crystallization of the polymer-rich phase. Both routes, that is, crystallization-controlled S-L TIPS on one side and L-L TIPS followed by polymer crystallization on the other side, seem suited for generation of polymer scaffolds with entrapped mosquito repellent.

✉ René Androsch
rene.androsch@iw.uni-halle.de

[1] Interdisciplinary Center for Transfer-oriented Research in Natural Sciences (IWE TFN), Martin Luther University Halle-Wittenberg, 06099 Halle/Saale, Germany

[2] Department of Engineering and Natural Sciences, University of Applied Sciences Merseburg, 06217 Merseburg, Germany

Regarding L-L TIPS followed by crystallization, successful scaffold formation was achieved by twin-screw extrusion of strands of poly (ethylene-*co*-vinyl acetate) (EVA) or linear low-density polyethylene (LLDPE) holding up to 30 m% DEET or Icaridin [19]. The homogeneous molten strand was guided into ice-water, allowing for L-L spinodal decomposition and solidification by polymer crystallization. Subsequent analysis of the evaporation characteristics of the repellents by foot-in-cage tests revealed protection against mosquitos up to after 12 weeks at 50 °C.

Similarly, binary solutions of LLDPE and the natural repellent citronellal (60 m%) were quenched from 150 °C to different sub-ambient temperatures between 5 and -170 °C, causing development of co-continuous polymer/repellent morphologies, however with negligible effect of the quenching temperature. The typical size of pores was less than a micron, and it was suggested that capillary forces effectively retain the liquid citronellal in the open pores [20].

In further studies, the polymer/repellent system poly(L-lactic acid) (PLLA)/DEET was investigated regarding the possibility to develop a biodegradable repellent-delivery device. PLLA dissolves in DEET above the polymer melting temperature and crystallizes from solution on cooling to below the equilibrium melting temperature [21–23]. PLLA scaffold formation during solution crystallization was successfully proven for solutions containing up to 50 m% PLLA, with typical pore sizes of the order of magnitude of few microns. In addition, it was found that PLLA/DEET solutions can be subject to electrospinning of fibers with a typical diameter of 1 μm and DEET loadings up to 50 m%, thus having the potential as a novel material for controlled release of DEET [24].

Though the polymer/repellent system PLLA/DEET is considered to be a promising drug-delivery device, there might remain disadvantages due to specific properties of the polymer component. PLLA is a rather slowly crystallizing polymer [25–28], with possible detrimental effects on the technology of producing such devices by classical melt-compounding, and perhaps even on the scaffold structure which is controlled by the number of crystal nuclei during solidification. Furthermore, despite being well-known for its environmental friendliness, PLLA degradation is rather slow [29–31], that is, improperly disposed PLLA-based drug-delivery devices will degrade at environmental conditions only over periods of months or even years [31]. For these reasons, in the present work, a further candidate for development of a polymer-based drug-delivery device, holding a mosquito repellent, is investigated. Poly(butylene succinate) (PBS) is a crystallizable polymer with a maximum possible crystallinity between 35 and 45% and exhibits a much higher crystallization rate than PLLA, it is bio-sourced, and the degradation rate is significantly faster [32–38]. PBS is commercially produced and gained importance in the fields of packaging, mulching films, or implants [38–40], and is also considered a base material for preparation of scaffold structures, to be applied, e.g., in bone tissue engineering [41–45]. Reports about its use as a drug/repellent carrier are not available.

Therefore, in the present study, the mixing behavior of PBS and DEET is investigated in order to evaluate the general possibility of the development of a scaffold-based drug-release tool aiming at repellence of mosquitos. In the first part, the solubility of the system components at elevated temperature as a prerequisite for crystallization-controlled TIPS during cooling is analyzed. This is followed by evaluation of the TIPS/crystallization conditions on the morphology of the system. In particular, the effects of the quenching/crystallization temperature and system composition to produce microporous structures from solutions are targeted, with the formed scaffolds advantageously imaged by scanning electron microscopy.

Experimental

Materials

The study was performed using an extrusion-grade PBS homopolymer produced by PTT MCC Biochem Co., Ltd. (Thailand) (www.pttmcc.com (accessed May 09, 2020)). The mass-average molar mass and polydispersity of the material are 123 kg/mol and 4.4, respectively (personal communication by MCPP-Europe (May 08, 2019)). DEET with a purity of 97 % was obtained from Sigma Aldrich (product number D100951) (https://www.sigmaaldrich.com/catalog/product/aldrich/d100951?lang=de&region=DE (accessed May 09, 2020)), and was used without any further purification. DEET is liquid at room temperature and exhibits a glass transition temperature of around -75 °C [21, 46]. Information about crystallization and melting are not available, and evaporation in thermogravimetry experiments revealed on heating at 5 K/min a mass loss of 10% at 180 °C [47]. As-received PBS pellets were dissolved in DEET at 150 °C in closed 4-mL glass vials while stirring, using a silicone oil bath. The prepared solutions contained 5, 10, 20, and 30 m% polymer.

Instrumentation

Cloud-point measurements

Cloud-point measurements were done to obtain temperatures of phase separation during slow cooling of the solutions. The solutions were kept in the closed 4-mL glass vials and cooled slower than 2 K/min using a silicone oil bath. During cooling, the transparency/turbidity of the solutions was monitored using a Leica digital microscope system DMS300 allowing for video recording.

Differential scanning calorimetry (DSC)

In addition to cloud-point measurements, DSC was employed for analysis of crystallization-controlled solid-liquid phase separation of solutions at higher cooling rates and improved temperature control. We used a heat-flux type DSC 1 from Mettler-Toledo connected to a Huber intracooler TC 100. Nitrogen gas with a flow rate of 60 mL/min was used as a purge gas to avoid thermo-oxidative degradation of the samples during the experiments. Solutions prepared as described above were transferred to 100-μL aluminum pans, with the sample mass being between 30 and 40 mg. To ensure that all crystals which may have formed during the transfer of the solutions with an initial temperature of 150 °C to the aluminum pan, samples were heated from the insert temperature of 25 °C to 150 °C and held at that temperature for 3 minutes before recording the cooling scans. All samples were used for recording of a single cooling scan only, in order to minimize the risk of a change of the polymer concentration due to evaporation of DEET on repeated heating.

Fast scanning differential scanning calorimetry (FSC)

FSC was used for analysis of the temperature dependence of the crystallization rate of PBS. We employed a power-compensation Flash DSC 1 from Mettler-Toledo, connected to a Huber TC100 intracooler. The sensor-support temperature was set to -90 °C, allowing for rapid cooling the melt to the desired crystallization temperatures. Nitrogen gas at a flow rate of 40 mL/min was used to purge the sample environment. Sample preparation included cutting of thin sections with a thickness of about 10 μm from the obtained pellets with the help of a Slee rotary microtome CUT 5062 equipped with a tungsten carbide knife. The thin sections were then reduced in their lateral size to about 50 μm under a stereomicroscope using a scalpel. Such specimens were then placed in the center of the heatable area of the sample calorimeter of the UFS 1 sensor, where a homogeneous temperature field has been proven in a separate study [48]. Prior to use and loading of the sample, the sensor was conditioned and temperature-corrected according to the instrument operating instructions.

Polarized-light optical microscopy (POM)

POM was used to confirm that TIPS during cooling solutions proceeded by polymer crystallization as well as for analysis of crystal-nuclei densities and rates of spherulite growth as a function of the crystallization conditions. A Leica DMRX microscope was operated in transmission mode with the samples placed between crossed polarizers. A droplet of the various PBS/DEET solutions was taken from the heated vials using a spatula, placed on a circular glass coverslip and covered by a second one. Then, the glass-sample-glass sandwich was placed into a Linkam THMS600 hot stage connected to a liquid-nitrogen accessory needed for fast cooling. Samples were heated to 150 °C and kept at this temperature for 1 min to melt crystals formed during sample preparation and to obtain a solution before the crystallization experiment. For analysis of isothermal crystallization, samples were cooled to selected temperatures at a rate of 100 K/min. A Motic 2300 CCD camera was used to capture images at a sampling rate of 5 s, in order to obtain spherulite growth rates.

Scanning electron microscopy (SEM)

SEM was employed for visualization of the microporous structure of PBS formed by crystallization-controlled TIPS of PBS/DEET solutions. A sufficient amount of solution was taken by a spatula from the vial and poured into an Anton Paar TTK sample chamber pre-conditioned at different temperatures between 0 and 60 °C, in order to obtain film-like samples with a thickness of 0.8 mm and scaffolds of different morphology. After isothermal crystallization, the samples were placed into an oven for 5 days at a temperature of 60 °C to evaporate the liquid DEET, before evaluation of the remained scaffold by a Tescan Vega 3 SBU SEM. The instrument was operated in a low-vacuum mode at a pressure of 10 Pa, using an acceleration voltage of 10 kV, avoiding the need for prior coating of the sample surface.

Results and discussion

Thermally induced phase separation and crystallization kinetics

PBS/DEET solutions were prepared at 160 °C and then subjected to a cloud-point analysis during slow cooling at a rate lower than 2 K/min, using a temperature sensor placed inside the solution. Figure 1 shows selected photographs of PBS/DEET mixtures containing 5, 10, 20, and 30 m% PBS (from left to right) taken at different temperatures between 150 °C (top row) and 60 °C (bottom row). The images of the upper row reveal absent turbidity at 150 °C regardless of the polymer concentration within the analyzed concentration range, indicating the presence of homogeneous solutions. During cooling, the first indication of turbidity was observed at about 70 °C in the sample with the highest PBS concentration of 30 m%. For the samples containing a lower amount of polymer of 20, 10, and 5 m%, cloud points are detected at lower temperatures of approximately 67, 65, and 63 °C, respectively. In general, cloudiness on cooling solutions may be caused by liquid-liquid or crystallization-induced solid-liquid phase separation, which, however, cannot be judged by visual inspection only. For this reason, calorimetry was employed as enthalpies of crystallization may be much larger than enthalpies of liquid-liquid

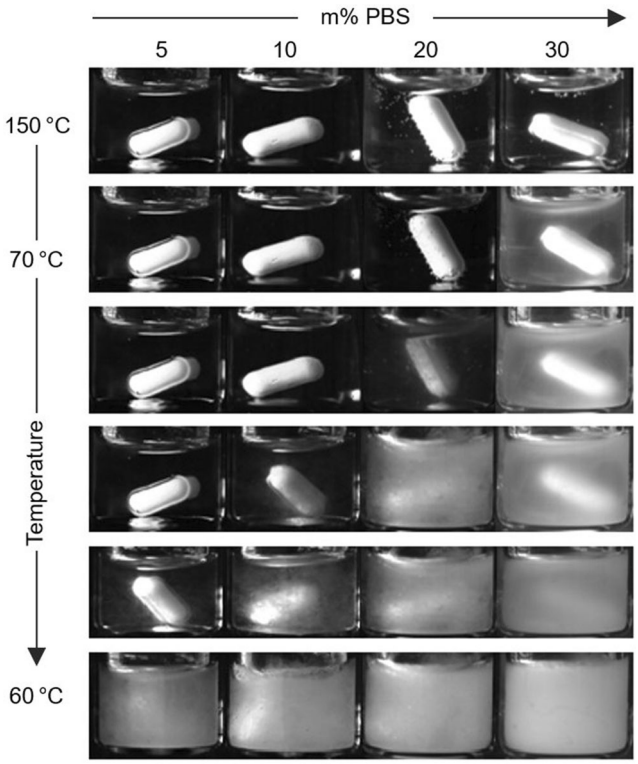

Fig. 1 Cloud-point analysis of PBS/DEET solutions containing between 5 m% (left column) and 30 m% PBS (right column). The photographs were taken at specific temperatures during slow cooling from 160 to 25 °C. The down-oriented arrow indicates the direction of the change of temperature

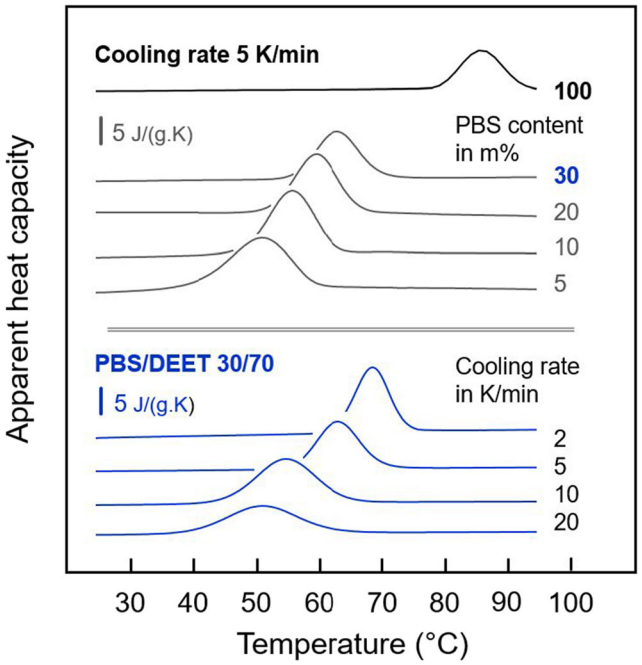

Fig. 2 DSC cooling scans of samples of PBS and PBS/DEET solutions containing different amounts of DEET, recorded using a rate of temperature change of 5 K/min (top part). The lower part shows DSC cooling scans of a PBS/DEET solution containing 30 m% polymer, recorded at different rates between 2 and 20 K/min. All curves were normalized to the actual polymer content

demixing, as concluded from former analysis of the polymer/solvent system PLLA/DEET [21]. Additionally, calorimetry served for more precise determination of phase-separation temperatures than is possible by eye.

Exemplary DSC cooling scans of PBS/DEET solutions in apparent-heat-capacity units are presented in Fig. 2, showing the effects of the polymer concentration on the temperature and enthalpy of crystallization during cooling at a constant rate of 5 K/min (top part), and of the cooling rate for a specific sample containing 30 m% polymer (bottom part). All data were normalized to the actual PBS content, allowing immediate judging of the crystallizability of PBS in the various solutions. Regarding the effect of the polymer concentration, neat PBS crystallizes on cooling at 5 K/min between about 80 and 90 °C, while crystallization of PBS in the presence of DEET occurs only at temperatures lower than about 70 °C, with the data revealing a systematic shift of the crystallization event to lower temperatures with increasing DEET content. Reasons for the lowering of the crystallization temperature of PBS when crystallizing from solutions may be a lowered equilibrium melting temperature [49] and the lowered polymer concentration, increasing diffusion pathways of molecular segments to the crystal growth front and slowing down the nucleation and crystallization rate [50–52]. In parallel, the enthalpy of PBS-crystallization (peak area) seems to increase slightly. For neat PBS, the enthalpy of crystallization is around 60 J/g which corresponds to a crystallinity of about 30% when using a value of 200 J/g for normalization [53, 54]. In case of crystallization of PBS in the presence of DEET, however, the PBS content-normalized enthalpy of crystallization is increased to yield PBS crystallinity values of around 50%, indicating, at least, that DEET does not hinder PBS crystallization from the point of view of the maximum achievable crystallinity. The possible reasons for the observed increased crystallinity are the reduced entanglement-density [55, 56] and/or absence of the rigid amorphous fraction both considered stopping melt crystallization when exceeding critical values [57].

In any case, the observation of exothermic peaks on cooling PBS/DEET solutions with an area of similar order of magnitude than in case of neat PBS we consider an important effect regarding the interpretation of the observed turbidity in the cloud-point experiments being mainly caused by crystallization and not by L-L phase separation. The latter would be connected with a much lower enthalpy of demixing. This view is supported by the typical, rather large effect of the cooling rate on the crystallization temperature, illustrated with the DSC curves in the lower part of Fig. 2. For (spinodal) L-L demixing of solutions, though also governed by time effects,

such distinct shift of the transition temperature with cooling rate is not expected [58, 59], as well as the peak area should not decrease with increasing cooling rate. However, it is important to note that the DSC and cloud-point experiments performed in the present work cannot provide a final answer whether crystallization is preceded or occurs in conjunction with L-L demixing. Such information may be obtained by suppressing the crystallization process as was done for the system PLA/DEET [21, 22].

Quantitative data about transition temperatures in non-isothermal crystallization experiments as a function of the PBS content are shown in Fig. 3. The various datasets, which are represented by different symbols/colors, demonstrate the effect of the cooling rate and reveal the above discussed kinetics of the crystallization process. The decrease of the crystallization temperature with increasing DEET concentration, in turn, is assumed being caused by the equilibrium-melting-temperature depression as well as the dilution effect, slowing down both homogeneous nucleation and growth of crystals [49–52].

Figure 4 shows overall crystallization rates in terms of crystallization half/peak times of neat PBS (gray symbols) and PBS crystallizing from solution (colored symbols) as a function of the crystallization temperature. Analysis of neat PBS allowed application of FSC, and with that it was possible to gain half/peak times of crystallization lower than about 1 min. Note that the kinetics of crystallization processes can only be quantified by DSC if exhibiting characteristic crystallization times of the order of magnitude slower than a minute, caused by the rather long instrumental time constant [60, 61]. The data obtained on neat PBS reveal that crystallization is fastest at around 45 °C, with the crystallization process completed within about 1 s at this temperature. This observation is

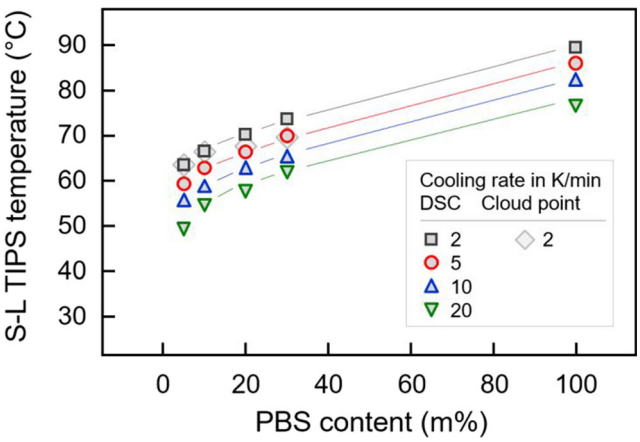

Fig. 3 DSC crystallization temperatures and cloud-point temperatures of PBS as a function of the PBS content in solutions with DEET. The different symbols and colors represent data obtained on cooling at different rates, as indicated in the legend. The lines serve as a guide for the eyes only

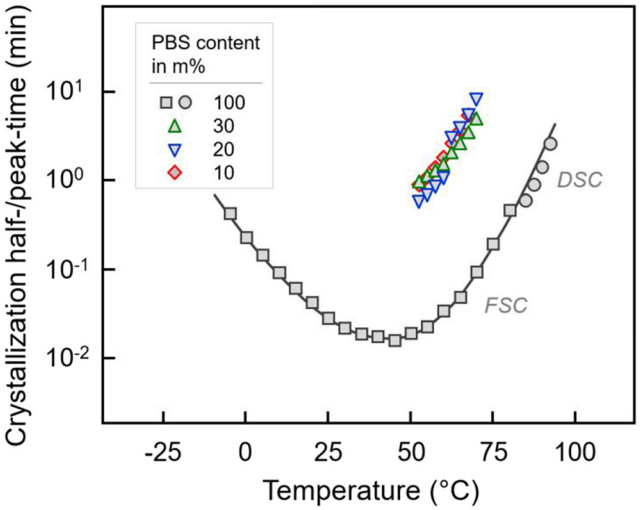

Fig. 4 Peak time (DSC) and half time of crystallization (FSC) of neat PBS (gray squares and circles) and PBS in solutions with DEET (colored symbols) as a function of temperature

in qualitative agreement with independent PBS crystallization studies [32, 34, 62], in which, however, different grades were investigated, serving as explanation for the observed differences. In contrast to neat PBS, PBS/DEET solutions were analyzed by DSC only, caused by the rather fast evaporation of DEET when attempting to prepare samples for FSC. Though the number of data is therefore largely reduced, it seems obvious that the crystallization temperature range is shifted to a lower temperature and that crystallization proceeds distinctly slower in the investigated range of temperature. This observation is in agreement with the non-isothermal experiments described with Figs. 2 and 3, and confirms a major effect of the presence of DEET on the kinetics of crystallization of PBS, despite a distinct influence of the DEET concentration was not detected within the analyzed range from 10 to 30 m% PBS.

Morphology and scaffold structure

Information about the semicrystalline morphology including scaffold structure formed during crystallization-controlled TIPS of PBS/DEET solutions were collected by POM and SEM. As an example, Fig. 5 shows optical micrographs of PBS/DEET samples containing 5, 10, 20, and 30 m% PBS (from left to right), cooled from 160 °C to ambient temperature at rates of 1, 5, 10, 50, and 100 K/min (from top to bottom). All images reveal a micrometer-scale structure consisting of rather isolated spherulites embedded in surrounding liquid. After TIPS on cooling, the latter is assumed to be a DEET-rich phase, while the spherulites are composed of solid PBS crystals surrounded/separated by amorphous PBS or a PBS-rich PBS/DEET solution.

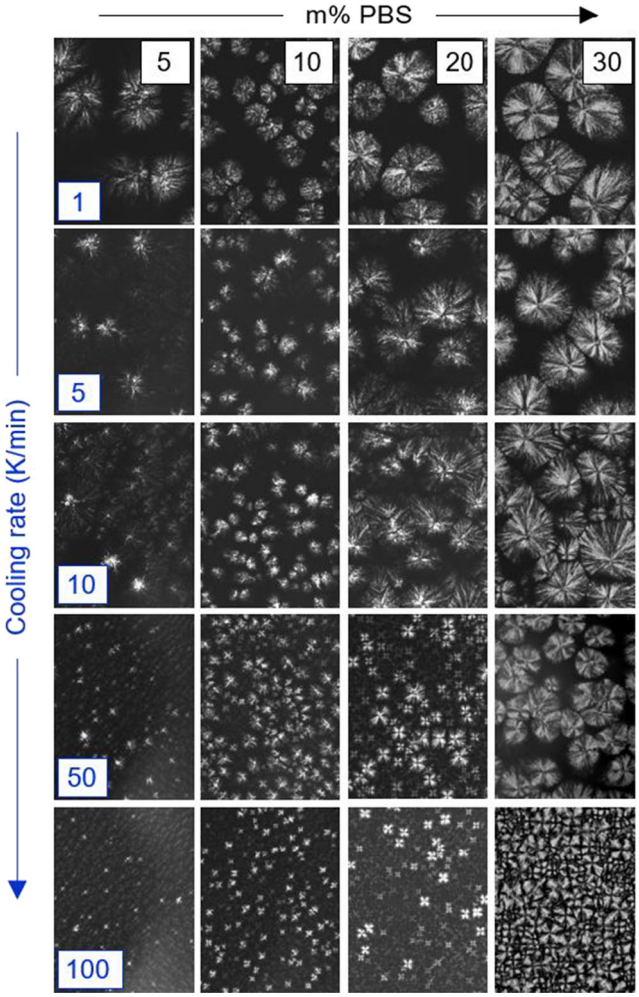

Fig. 5 Spherulitic superstructure of PBS/DEET samples containing 30, 20, 10, and 5 m% PBS (right to left), non-isothermally crystallized at rates of 1, 5, 10, 50, and 100 K/min (from top to bottom)

Regarding the effect of the cooling rate on crystallization, as expected from the general dependence of the nucleation rate on temperature [63, 64], there is an increasing number of nuclei/spherulites observed when increasing the cooling rate, that is, if nucleation/crystallization occurs at higher supercooling. Regarding the effect of the polymer concentration, it is obvious that a larger number of spherulites/crystalline fraction is detected when increasing the polymer content. Though not in foreground in the present study, from the point-of-view of a possible application of the PBS/DEET system as a drug/repellent-delivery device, the POM micrographs lead to the conclusion that intermeshing of spherulites, in order to obtain mechanical stability instead of a rather liquid-like behavior, is only observed for samples containing 30 m% polymer, and after fast cooling. On the other side, even liquid-/gel-like behaving compounds of high concentration of the active ingredient may find application when combined with a stabilizing surrounding structure, for example, skin layer, generated in extrusion or fiber spinning processes [19, 65, 66].

Further information about the structure of solidified samples were gained by SEM, additionally revealing intra-spherulitic features. Before SEM imaging, the liquid solvent-rich phase was removed by evaporation in a vacuum oven, operated at 60 °C. Figure 6 shows the structure of a sample which initially contained 30 m% PBS, and which was subjected to crystallization-controlled TIPS at temperatures of 0 (top row), 30 (center row), and 60 °C (bottom row), at different magnifications. In agreement with the POM micrographs of Fig. 5, obtained on a rapidly cooled sample crystallized at a low temperature (bottom right image), TIPS at 0 °C led to a space-filled spherulitic morphology, that is, the liquid DEET-rich phase (> 70 m%) is incorporated in the spherulites. In particular, the image obtained at higher magnification (top right) reveals intra-spherulitic pores in which DEET is hosted. At higher crystallization temperatures of 30 and 60 °C, spherulites are not space filling anymore, that is, the DEET-rich phase is additionally located outside the spherulites. Again, the higher resolution images of the right column in Fig. 6 provide information about the structure of the solid intra-spherulitic scaffold formed by lamellar PBS crystals. Furthermore, the soft zoom of the sample crystallized at 30 °C, shown in Fig. 7, allows estimation of the size of the intra-spherulitic pores being of the order of magnitude of a micrometer, or smaller.

Conclusions

The present work served for evaluation whether it is possible to generate a polymeric scaffold based on biosourced and biodegradable poly(butylene succinate) (PBS), to be used as a reservoir for the mosquito-repellent *N*,*N*-diethyl-3-methylbenzamide (DEET). The prerequisite for formation of a microporous polymer scaffold is the solubility of the system components which has successfully been proven for the selected polymer, when dissolution is performed at temperatures higher than the PBS melting temperature (see Fig. 1). Crystallization-controlled thermally induced phase separation and the formation of a spherulitic superstructure occur on cooling the solutions, with the morphology depending on the cooling conditions (see Fig. 5). A rather space-filled spherulitic morphology is obtained on fast cooling, implying fast crystallization at a rather low temperature (see Figs. 2, 3, and 4), and if the polymer content is sufficiently high, being larger than about 20 m% PBS (see Figs. 6 and 7). In that case, the liquid DEET-rich phase is located in intra-spherulitic pores with a size of the order of micrometers or even smaller. As such, the performed study provides a

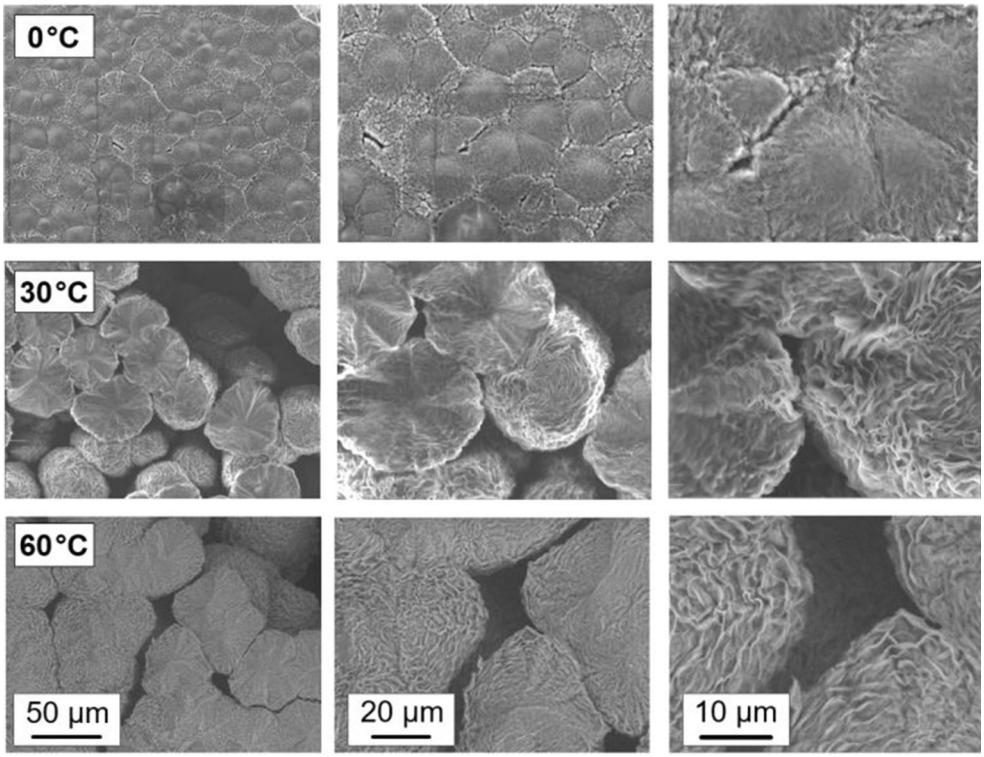

Fig. 6 SEM micrographs of PBS/DEET samples initially containing 30 m% PBS, crystallized at 0 (top), 30 (center), and 60 °C (bottom), taken at different magnifications

basis for further research activities in the field of development of repellent-release devices using biodegradable PBS as carrier for environment-friendly after-use disposal.

Acknowledgments The authors thank MCPP Germany GmbH for supplying the polymer. We also thank Olaf Krimig and Denis Wiegandt for their assistance with the SEM.

Funding Open Access funding enabled and organized by Projekt DEAL. HEY and RA received financial support from the Deutsche Forschungsgemeinschaft (DFG) (Grant number AN 212/22).

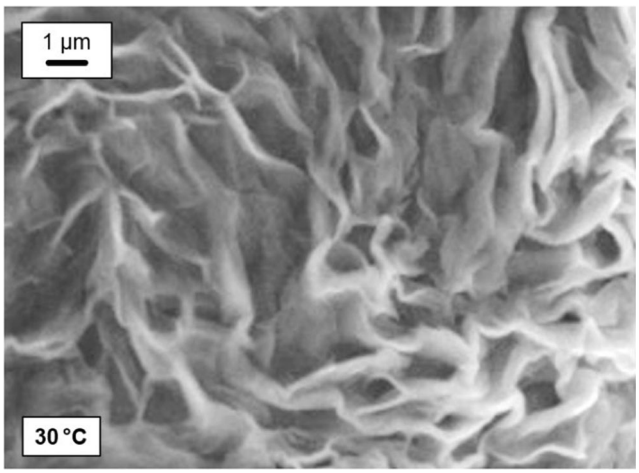

Fig. 7 Soft zoom of an SEM micrograph of a PBS/DEET sample initially containing 30 m% PBS, crystallized at 30 °C

Compliance with ethical standards

Conflict of interest The authors declare that they have no conflict of interest.

References

1. World malaria report 2019. Geneva: World Health Organization; 2019. License: CC BY-NC-SA 3.0 IGO.
2. Roberts JR, Reigart JR (2004) Does anything beat DEET? Pediatr Ann 33:444–453
3. Fradin MS, Day JF (2002) Comparative efficacy of insect repellents against mosquito bites. N Engl J Med 347:13–18
4. Fradin MS (1998) Mosquitoes and mosquito repellents: a clinician's guide. Ann Intern Med 128:931–940
5. N'Guessan R, Knols BG, Pennetier C, Rowland M (2008) DEET microencapsulation: a slow-release formulation enhancing the

residual efficacy of bed nets against malaria vectors. Trans R Soc Trop Med Hyg 102:259–262
6. Cecone C, Caldera F, Trotta F, Bracco P, Zanetti M (2018) Controlled release of DEET loaded on fibrous mats from electrospun PMDA/cyclodextrin polymer. Molecules 23:1694
7. Barradas TN, Lopes LMA, Ricci-Júnior E, e Silva KGDH, Mansur CRE (2013) Development and characterization of micellar systems for application as insect repellents. Int J Pharm 454:633–640
8. Rutledge LC, Gupta RK, Mehr ZA, Buescher MD, Reifenrath WG (1996) Evaluation of controlled-release mosquito repellent formulations. J Am Mosq Control Assoc 12:39–44
9. Gupta RK, Sweeney AW, Rutledge LC, Cooper RD, Frances SP, Westrom DR (1987) Effectiveness of controlled-release personal-use arthropod repellents and permethrin-impregnated clothing in the field. J Am Mosq Control Assoc 3:556–660
10. Emam HE, Abdelhameed RM (2017) In-situ modification of natural fabrics by Cu-BTC MOF for effective release of insect repellent (N, N-diethyl-3-methylbenzamide). J Porous Mater 24:1175–1185
11. Nam YS, Park TG (1999) Porous biodegradable polymeric scaffolds prepared by thermally induced phase separation. J Biomed Mater Res 47:8–17
12. Hua FJ, Kim GE, Lee JD, Son YK, Lee DS (2002) Macroporous poly(L-lactide) scaffold 1. Preparation of a macroporous scaffold by liquid–liquid phase separation of a PLLA–dioxane–water system. J Biomed Mater Res 63:161–167
13. Yang F, Murugan R, Ramakrishna S, Wang X, Ma Y-X, Wang S (2004) Fabrication of nano-structured porous PLLA scaffold intended for nerve tissue engineering. Biomaterials 25:1891–1900
14. Mohammadi MS, Bureau MN, Nazhat SN (2014) Polylactic acid (PLA) biomedical foams for tissue engineering. In: Biomedical Foams for Tissue Engineering Applications. Woodhead Publishing, pp 313–334
15. Schugen C, Maquet V, Grandfils C, Jerome R, Teyssie P (1996) Biodegradable and macroporous polylactide implants for cell transplantation: 1. Preparation of macroporous polylactide supports by solid-liquid phase separation. Polymer 37:1027–1038
16. Önder ÖC, Yilgör E, Yilgör I (2016) Fabrication of rigid poly(lactic acid) foams via thermally induced phase separation. Polymer 107: 240–248
17. Lloyd DR, Kinzer KE, Tseng HS (1990) Microporous membrane formation via thermally induced phase separation. I. Solid-liquid phase separation. J Membr Sci 52:239–261
18. Lloyd DR, Kim SS, Kinzer KE (1990) Microporous membrane formation via thermally induced phase separation. II. Liquid-liquid phase separation. J Membr Sci 64:1–11
19. Mapossa AB, Sibanda MM, Sitoe A, Focke WW, Braack L, Ndonyane C, Mouatcho J, Smart J, Muaimbo H, Androsch R, Loots MT (2019) Microporous polyolefin strands as controlled-release devices for mosquito repellents. Chem Eng J 360:435–444
20. Akhtar MU, Focke WW (2015) Trapping citronellal in a microporous polyethylene matrix. Thermochim Acta 613:61–65
21. Sungkapreecha C, Iqbal N, Gohn AM, Focke WW, Androsch R (2017) Phase behavior of the polymer/drug system PLA/DEET. Polymer 126:116–125
22. Sungkapreecha C, Beily MJ, Kressler J, Focke WW, Androsch R (2018) Phase behavior of the polymer/drug system PLA/DEET: Effect of PLA molar mass on subambient liquid-liquid phase separation. Thermochim Acta 660:77–81
23. Sungkapreecha C, Iqbal N, Focke WW, Androsch R (2019) Crystallization of poly (L-lactic acid) in solution with the mosquito-repellent N,N-diethyl-3-methylbenzamide. Polym Crystallization 2:e10029
24. Bonadies I, Longo A, Androsch R, Jehnichen D, Göbel M, Di Lorenzo ML (2019) Biodegradable electrospun PLLA fibers containing the mosquito-repellent DEET. Eur Polym J 113:377–384
25. Vasanthakumari R, Pennings AJ (1983) Crystallization kinetics of poly (L-lactic acid). Polymer 24:175–178
26. Di Lorenzo ML (2005) Crystallization behavior of poly (L-lactic acid). Eur Polym J 41:569–575
27. Saeidlou S, Huneault MA, Li H, Park CB (2012) Poly (lactic acid) crystallization. Prog Polym Sci 37:1657–1677
28. Androsch R, Schick C, Di Lorenzo ML (2017) Kinetics of nucleation and growth of crystals of poly (L-lactic acid). Adv Polym Sci 279:235–272. https://doi.org/10.1007/12_2016_13
29. Gorrasi G, Pantani R (2017) Hydrolysis and Biodegradation of Poly(lactic acid). Adv Polym Sci 279:119–151. https://doi.org/10.1007/12_2016_12
30. Zhang X, Wyss UP, Pichora D, Goosen MF (1994) An investigation of poly (lactic acid) degradation. J Bioact Compat Polym 9:80–100
31. Garlotta D (2001) A literature review of poly (lactic acid). J Polym Environ 9:63–84
32. Papageorgiou GZ, Achilias DS, Bikiaris DN (2007) Crystallization kinetics of biodegradable poly (butylene succinate) under isothermal and non-isothermal conditions. Macromol Chem Phys 208: 1250–1264
33. Gan Z, Abe H, Kurokawa H, Doi Y (2001) Solid-state microstructures, thermal properties, and crystallization of biodegradable poly (butylene succinate) (PBS) and its copolyesters. Biomacromolecules 2:605–613
34. Jiang J, Zhuravlev E, Hu WB, Schick C, Zhou DS (2017) The effect of self-nucleation on isothermal crystallization kinetics of poly (butylene succinate) (PBS) investigated by differential fast scanning calorimetry. Chin J Polym Sci 35:1009–1019
35. Piorkowska E (2019) Overview of Biobased Polymers. Adv Polym Sci 283:1–35. https://doi.org/10.1007/12_2019_52
36. Su S, Kopitzky R, Tolga S, Kabasci S (2019) Polylactide (PLA) and its blends with poly (butylene succinate)(PBS): A brief review. Polymers 11:1193
37. Adhikari D, Mukai M, Kubota K, Kai T, Kaneko N, Araki KS, Kubo M (2016) Degradation of bioplastics in soil and their degradation effects on environmental microorganisms. J Agric Chem Environ 5:23–34
38. Xu J, Guo BH (2010) Poly (butylene succinate) and its copolymers: research, development and industrialization. Biotechnol J 5:1149–1163
39. Siracusa V, Lotti N, Munari A, Dalla Rosa M (2015) Poly (butylene succinate) and poly (butylene succinate-co-adipate) for food packaging applications: Gas barrier properties after stressed treatments. Polym Degrad Stab 119:35–45
40. Xu J, Guo BH (2010) Microbial succinic acid, its polymer poly (butylene succinate), and applications. Plastics from Bacteria. Springer, Berlin, Heidelberg, pp 347–388
41. Gigli M, Fabbri M, Lotti N, Gamberini R, Rimini B, Munari A (2016) Poly (butylene succinate)-based polyesters for biomedical applications: A review. Eur Polym J 75:431–460
42. Ju J, Gu Z, Liu X, Zhang S, Peng X, Kuang T (2020) Fabrication of bimodal open-porous poly (butylene succinate)/cellulose nanocrystals composite scaffolds for tissue engineering application. Int J Biol Macromol 147:1164–1173
43. Cristofaro F, Gigli M, Bloise N, Chen H, Bruni G, Munari A, Moroni L, Lotti N, Visai L (2018) Influence of the nanofiber chemistry and orientation of biodegradable poly (butylene succinate)-based scaffolds on osteoblast differentiation for bone tissue regeneration. Nanoscale 10:8689–8703
44. Zhang D, Chang J, Zeng Y (2008) Fabrication of fibrous poly (butylene succinate)/wollastonite/apatite composite scaffolds by electrospinning and biomimetic process. J Mater Sci Mater Med 19:443–449
45. Wu Z, Zheng K, Zhang J, Tang T, Guo H, Boccaccini AR, Wei J (2016) Effects of magnesium silicate on the mechanical properties,

biocompatibility, bioactivity, degradability, and osteogenesis of poly (butylene succinate)-based composite scaffolds for bone repair. J Mater Chem B4:7974–7988
46. Griffin PJ, Sangoro JR, Wang Y, Holt AP, Novikov VN, Sokolov AP, Wojnarowska Z, Paluch M, Kremer F (2013) Dynamic crossover and the Debye–Stokes–Einstein relation in liquid N, N-diethyl-3-methylbenzamide (DEET). Soft Matter 9:10373–10380
47. Annandarajah C, Norris EJ, Funk R, Xiang C, Grewell D, Coats JR, Mishek D, Maloy B (2019) Biobased plastics with insect-repellent functionality. Polym Eng Sci 59:E460–E467
48. Jariyavidyanont K, Abdelaziz A, Androsch R, Schick C (2019) Experimental analysis of lateral thermal inhomogeneity of a specific chip-calorimeter sensor. Thermochim Acta 674:95–99
49. Flory PJ (1949) Thermodynamics of crystallization in high polymers. IV. A theory of crystalline states and fusion in polymers, copolymers, and their mixtures with diluents. J Chem Phys 17: 223–240
50. Martuscelli E (1984) Influence of composition, crystallization conditions and melt phase structure on solid morphology, kinetics of crystallization and thermal behavior of binary polymer/polymer blends. Polym Eng Sci 24:563–586
51. Sanchez IC, Eby RK (1975) Thermodynamics and crystallization of random copolymers. Macromolecules 8:638–641
52. Lauritzen Jr JI, Hoffman JD (1960) Theory of formation of polymer crystals with folded chains in dilute solution. J Res Nat Bur Stand Sect A Phys Chem 64:73
53. Miyata T, Masuko T (1998) Crystallization behaviour of poly (tetramethylene succinate). Polymer 39:1399–1404
54. Papageorgiou GZ, Bikiaris DN (2005) Crystallization and melting behavior of three biodegradable poly (alkylene succinates). A comparative study. Polymer 46:12081–12092
55. Luo C, Sommer JU (2014) Frozen topology: Entanglements control nucleation and crystallization in polymers. Phys Rev Lett 112: 195702
56. Kurz R, Schulz M, Scheliga F, Men Y, Seidlitz A, Thurn-Albrecht T, Saalwächter K (2018) Interplay between crystallization and entanglements in the amorphous phase of the crystal-fixed polymer poly (ϵ-caprolactone). Macromolecules 51:5831–5841
57. Wunderlich B (2012) Termination of crystallization or ordering of flexible, linear macromolecules. J Therm Anal Calorim 109:1117–1132
58. Bae YC, Lambert SM, Soane DS, Prausnitz JM (1991) Cloud-point curves of polymer solutions from thermooptical measurements. Macromolecules 24:4403–4407
59. Mannella GA, La Carrubba V, Brucato V (2013) Measurement of cloud point temperature in polymer solutions. Rev Sci Instrum 84: 075118
60. Turnbull D, Fisher JC (1949) Rate of nucleation in condensed systems. J Chem Phys 17:71–73
61. Schick C, Androsch R, Schmelzer JWP (2017) Homogeneous crystal nucleation in polymers. J Phys Condens Matter 29:453002
62. Papageorgiou DG, Zhuravlev E, Papageorgiou GZ, Bikiaris D, Chrissafis K, Schick C (2014) Kinetics of nucleation and crystallization in poly (butylene succinate) nanocomposites. Polymer 55: 6725–6734
63. Höhne GWH, Hemminger W (1996) Flammersheim HJ (2013) Differential Scanning Calorimetry: An Introduction for Practitioner. Springer, Berlin
64. Androsch R (2000) Heat capacity measurements using temperature-modulated heat flux DSC with close control of the heater temperature. J Therm Anal Calorim 61:75–89
65. Sibanda M, Focke W, Braack L, Leuteritz A, Brünig H, Tran NHA, Wieczorek F, Trümper W (2018) Bicomponent fibres for controlled release of volatile mosquito repellents. Mater Sci Eng C 91:754–761
66. Naeimirad M, Zadhoush A, Kotek R, Esmaeely Neisiany R, Nouri Khorasani S, Ramakrishna S (2018) Recent advances in core/shell bicomponent fibers and nanofibers: A review. J Appl Polym Sci 135:46265